



AALBORG UNIVERSITY
DENMARK

Aalborg Universitet

MIMO OTA Testing in Small Multi-Probe Anechoic Chamber Setups

Llorente, Ines Carton; Fan, Wei; Pedersen, Gert F.

Published in:

I E E Antennas and Wireless Propagation Letters

DOI (link to publication from Publisher):

[10.1109/LAWP.2015.2497542](https://doi.org/10.1109/LAWP.2015.2497542)

Publication date:

2016

Document Version

Accepted author manuscript, peer reviewed version

[Link to publication from Aalborg University](#)

Citation for published version (APA):

Llorente, I. C., Fan, W., & Pedersen, G. F. (2016). MIMO OTA Testing in Small Multi-Probe Anechoic Chamber Setups. *I E E Antennas and Wireless Propagation Letters*, 15, 1167 - 1170. Advance online publication. <https://doi.org/10.1109/LAWP.2015.2497542>

General rights

Copyright and moral rights for the publications made accessible in the public portal are retained by the authors and/or other copyright owners and it is a condition of accessing publications that users recognise and abide by the legal requirements associated with these rights.

- Users may download and print one copy of any publication from the public portal for the purpose of private study or research.
- You may not further distribute the material or use it for any profit-making activity or commercial gain
- You may freely distribute the URL identifying the publication in the public portal -

Take down policy

If you believe that this document breaches copyright please contact us at vbn@aub.aau.dk providing details, and we will remove access to the work immediately and investigate your claim.

MIMO OTA Testing in Small Multi-Probe Anechoic Chamber Setups

Inés Cartón Llorente, Wei Fan, Gert F. Pedersen

Abstract—Over the Air (OTA) testing of MIMO capable terminals is often performed in large anechoic chambers, where planar waves impinging the test area are assumed. Furthermore, reflections from the chamber, and probe coupling are often considered negligible due to the large dimensions of the chamber. This paper investigates the feasibility of reducing the physical dimension of 2D multi-probe anechoic chamber setups for MIMO OTA testing, with the purpose of reducing the cost and space of the setup. In the paper, a channel emulation algorithm and chamber compensation technique are proposed for MIMO OTA testing in small anechoic chambers. The performance deterioration in a small anechoic chamber, i.e., with a ring radius of 0.5 m, is demonstrated via simulations.

Index Terms—Channel Emulation, MIMO OTA testing, small multi-probe anechoic chamber setup, test area sampling.

I. INTRODUCTION

THE purpose of Over the Air (OTA) testing is to assess the performance of wireless devices including antenna performance. MIMO capable devices should be tested under realistic channel conditions, so that its true performance is assessed. The multi-probe anechoic chamber (MPAC) method is a promising solution to achieve this. In this method, a number of source antennas, referred to as probe antennas, are placed inside an anechoic chamber surrounding the Device Under Test (DUT). Through the use of a channel emulator connected to the probe antennas, various spatial channels can be created [1]. The main disadvantage of the MPAC method is its cost. A sufficient number of probe antennas is required to accurately emulate the channel, which leads to costly designs [2]. In addition, the radius of the ring where the probes are placed is typically assumed to be sufficiently large so that waves radiated from the probe antennas are planar in the test area. Typical ring radius in practical OTA setups reported in the literature is, for example, 2 m in Aalborg University and ETS-Lindgren setups, to name a few [3]. A large multi-probe setup and consequently a large anechoic chamber are often cost-prohibitive.

There is an increasing interest from the industry to have a cost-effective MPAC setup by building a space-saving, flexible and portable system. An attempt in this direction is the commercial solution in [4] with a ring radius of 1.2 m. A compact and portable system is advantageous because laboratory space is often valuable and limited. Methods to reduce the physical dimensions of MPAC setups used for MIMO OTA testing while still accurately emulating desired radio channels are highly desirable. As the size of the setup is reduced, the waves radiated from the probe antennas become spherical. Furthermore, reflections and probe coupling might become a concern. The measurement uncertainty increases with probe

coupling as demonstrated in [5]. Results in [6] indicate that reflections from the chamber significantly affect the quality of the quiet zone in small setups. This paper investigates such effects on the channel emulation accuracy in small MPAC setups. We refer to “small” MPAC setups as those where the radiated waves cannot be considered planar.

One of the major challenges in OTA testing is to emulate the desired environment by controlling the signals radiated from the probes. The Prefaded Signals Synthesis (PFS) technique is one of the channel emulation techniques that has gained popularity in commercial products [1]. The PFS technique aims at reproducing Geometrically Based Stochastic Channel (GBSC) models, by transmitting prefaded signals with specific power weights from the probes [1]. For the PFS technique, it is typically assumed that the signals have planar wavefront. However, this assumption might not be valid in small MPAC setups. Paper [7] provides theoretical errors due to the proximity between the DUT and the probes, yet channel emulation was not addressed. In this paper, we revise the PFS technique and propose a new way to sample the test zone appropriate for chambers of any size.

The main contribution of this paper is to study the feasibility of emulating GBSC models using the PFS method in small MPAC setups for MIMO OTA testing. To enable this, we have investigated different aspects:

- A method for channel emulation in small MPAC setups using the PFS technique is proposed in Section II. This includes novel methods to sample the test area that take into account the spherical wave effect and are suitable for chambers of arbitrary sizes.
- A chamber compensation technique is proposed to minimize reflections and probe coupling in MPAC setups.
- Channel emulation accuracy deterioration due to spherical waves, reflections and coupling in small MPACs are shown in Section IV, along with simulations validating the previous contributions for different channel models.

II. CHANNEL EMULATION IN SMALL MPAC SETUPS

The main contributions of this part lies in two aspects: an extension of the PFS technique and a novel test area sampling method to make the PFS technique suitable for chambers of arbitrary size. GBSC models specify a continuous Power Angular Spectrum (PAS) at the receiver side. The focus of the PFS technique is to reconstruct the target PAS with a limited number of probes [8].

A. Target Spatial Correlation

The target spatial correlation ρ between a pair of antennas depends on the target continuous PAS and complex patterns of

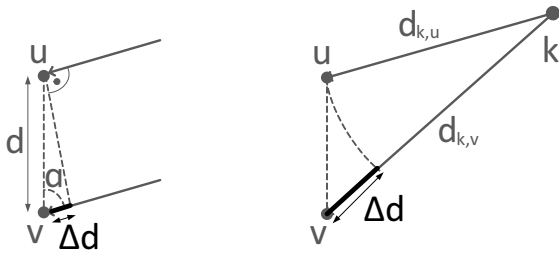


Fig. 1. Wave generated by the k -th probe antenna impinging antennas u and v , for planar wave assumption (left), and spherical wave (right). The phase difference between u and v depends on the path length difference Δd .

the antennas [1]. Since the patterns of the DUT antennas are unknown, they are often assumed to be omnidirectional with a phase difference dependent on the antenna separation [1], [8]. The target correlation is:

$$\rho = \int_{-\pi}^{\pi} \exp(j2\pi d \cos(\alpha)/\lambda) P(\phi) d\phi \quad (1)$$

where λ is the carrier wavelength, d , α are shown in Fig. 1, and $P(\phi)$ is the target PAS, composed of ideal plane waves [1].

B. Emulated Spatial Correlation

The emulated spatial correlation $\hat{\rho}$ generated by a limited number of probe antennas K , for ideal MPAC setups is [1]:

$$\hat{\rho}_{ideal} = \sum_{k=1}^K g_k \cdot \exp(j2\pi d \cos(\alpha)/\lambda) \quad (2)$$

where g_k is the power weight for the k -th probe antenna. The emulated correlation for small chambers should include the phase and gain errors produced by spherical waves [7]:

$$\hat{\rho}_{small} = \frac{\sum_{k=1}^K g_k \cdot F_{k,u} F_{k,v} \exp(j2\pi(d_{k,u} - d_{k,v})/\lambda)}{\sqrt{\sum_{k=1}^K F_{k,u}^2 g_k \cdot \sum_{k=1}^K F_{k,v}^2 g_k}} \quad (3)$$

where $F_{k,u}$, $F_{k,v}$ are the path loss terms from probe k to antennas u , v , and $d_{k,u}$, $d_{k,v}$ are shown in Fig. 1. Note that (2) is a special case of (3) with the probes placed sufficiently far.

C. Objective Function

The objective is to obtain the probe weights $\mathbf{g} = \{g_k\}$, $g_k \in [0, 1]$ with $k = 1, \dots, K$, to minimize the error between the target spatial correlation $\boldsymbol{\rho} = \{\rho_1, \dots, \rho_M\}$ and the emulated spatial correlation $\hat{\boldsymbol{\rho}} = \{\hat{\rho}_1, \dots, \hat{\rho}_M\}$ over M antenna pairs [8]:

$$\min_{\mathbf{g}} \|\boldsymbol{\rho} - \hat{\boldsymbol{\rho}}_{small}(\mathbf{g})\|^2 \quad (4)$$

where \mathbf{g} is obtained by applying convex optimization to (4) [8].

D. Test Area Sampling

In ideal MPAC setups, M antenna pairs are selected to sample the test area as opposite points on circles of different radius [8] as shown in Fig. 2 (left). However, the selected antenna pairs are always symmetric with respect to the center, which is not representative of the test area samples in small setups, as demonstrated in Section IV. Instead, the test area should be sampled by pairs of antennas that represent all

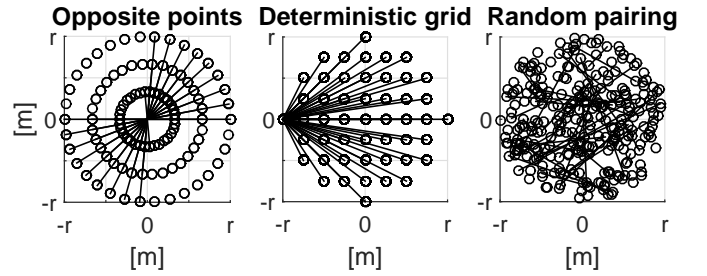


Fig. 2. Test area sampling methods. The circles represent the position of the antennas, and the lines show how these antennas would be paired. Note that only few antenna pairs are shown for illustration purpose.

possible locations of the DUT antennas, so that spherical wave effects are taken into account. Two sampling methods are proposed in this paper, namely random pairing and deterministic grid pairing, illustrated in Fig. 2. The former consists on pairing antennas randomly placed inside the test area. In the later, the antennas are located on a square grid covering the test area and combinations of any two samples are paired.

III. CHAMBER COMPENSATION TECHNIQUE

In this section, we consider the case where the system is no longer ideal, i.e., reflections and coupling between the probes affect channel emulation. In this case, the field within the test area includes both the desired signals from the probes and the undesired signals caused by reflections and coupling between the probes. By identifying the strength and direction of the undesired paths, we can build a chamber model that can be pre-compensated to reduce undesired signals in the channel emulation stage. We assume that the dominant sources of error are reflections and coupling between the probes, whereas coupling between the probes and the DUT is considered negligible. The proposed technique is inspired by the work in [9], where the goal was to compensate near-field effects and scattering contributions from neighboring probes.

A. Chamber Model

An antenna with an omnidirectional pattern, e.g., a calibration dipole, can be used to create the chamber model. The calibration antenna is swept over P positions on a circle of radius equal to the target test area radius r , as shown in Fig. 3, to identify the incoming direction of undesired and desired paths. The minimum number of calibrating positions required is $P = K$. The S_{21} is measured using a network analyzer for each antenna position with each probe antenna active at a time, leading to the chamber model \mathbf{S} which is a complex matrix of size $P \times K$. Note that the reflection coefficient is frequency dependent. Therefore, the chamber model needs to be measured for each frequency band to be tested.

B. Compensation Technique

Knowing the geometric position of the probe antennas and the calibration antenna, the target field $\mathbf{T} \in \mathbb{C}^{P \times K}$ for each active probe antenna can be calculated. The goal is to calculate the weights $\mathbf{D} \in \mathbb{C}^{K \times K}$ that compensate the undesired paths in \mathbf{S} , while maintaining the desired (target) ones:

$$\mathbf{S} \cdot \mathbf{D} = \mathbf{T} \quad (5)$$

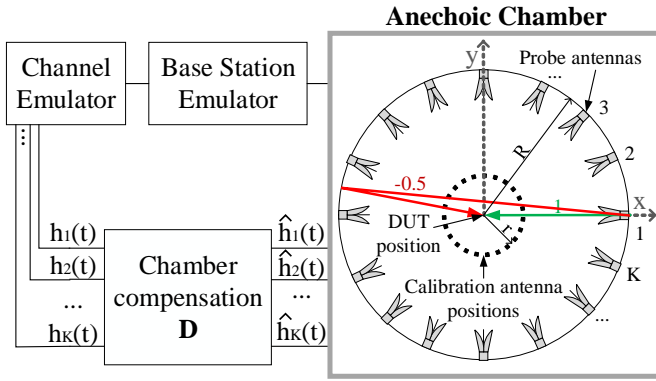


Fig. 3. MPAC setup including chamber compensation. K probe antennas are placed on a ring of radius R , surrounding the test area of radius r . The DUT would be placed in the center of the chamber since its antennas must be within the test area during performance testing. A reflection produced by the ring, incoming from in between two probes due to probe 1 being active is shown.

Using the Moore-Penrose pseudoinverse, (5) is solved as:

$$\mathbf{D} = (\mathbf{S}^H \mathbf{S})^{-1} \mathbf{S}^H \mathbf{T} \quad (6)$$

where $(\cdot)^H$ is the hermitian transpose. Note that both the target field and the measured field include the spherical wave effect. The procedure would minimize reflections and coupling on the azimuth plane only. Reflections from other elevation angles are assumed to be negligible, as absorbers would be placed on the walls in practical setups. Fig. 3 shows the idea of the chamber compensation in a MPAC setup.

For a single cluster, the spatial channel characteristics are achieved by weighting the coefficients with the optimized weights \sqrt{g} [1]. To compensate for undesired effects in the chamber, we multiply the channel coefficients $h_k(t)$ by matrix \mathbf{D} , obtaining the compensated coefficients $\hat{h}_k(t)$:

$$\hat{h}_k(t) = \sum_{n=1}^K D_{k,n} \cdot h_n(t) \quad (7)$$

where $D_{k,n}$ corresponds to the element in row k and column n of matrix \mathbf{D} . The compensated channel coefficients are a linear combination of the original ones. For channel models composed by multiple clusters, each cluster is emulated individually and independently [8]. The chamber compensation technique is applied to each cluster independently as well.

IV. SIMULATION RESULTS

In the following results, a small MPAC setup with ring radius 0.5 m and a test area of diameter 0.2 m is considered.

A. Validation of Test Area Sampling Methods

We use the deviation between the target spatial correlation calculated from an ideal PAS, i.e., using (1), and the simulated correlation for the same PAS in a small chamber. The deviation depends on the location of the pair antennas and the target PAS [7]. Table I shows the deviation for four representative PASs. Note that the error is exclusively caused by spherical wave effect. The method proposed in [8] fails to represent the actual error over the test area. On the other hand, the other two methods proposed in this paper are more suitable. Both

TABLE I
RMS CORRELATION ERROR FOR DIFFERENT SAMPLING METHODS.

	Opposite points on a circle	Random pairing	Grid sampling
Uniform PAS	0.007	0.061	0.056
Laplacian (AS = 35°)	0.007	0.070	0.070
SCME-Umi	0.009	0.072	0.065
SCME-Uma	0.008	0.066	0.061

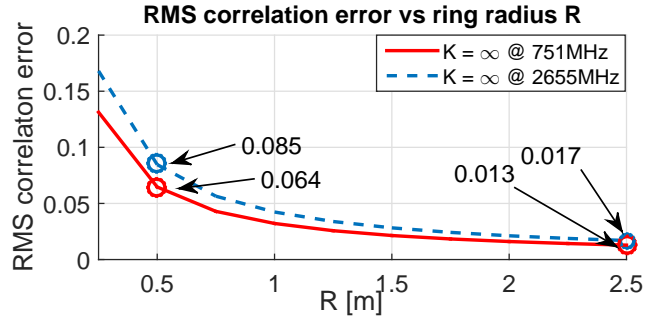


Fig. 4. RMS error for the SCME Urban micro model as a function of R . Deviation values for $R=0.5$ m and $R=2.5$ m are marked.

methods achieve similar results, yet the grid pairing has the advantage of being deterministic.

B. Spherical Wave Effect

Fig. 4 shows the RMS deviation as a function of the ring radius R for two representative frequencies: 751 MHz and 2655 MHz, central frequencies of LTE bands 13 and 7. The error is caused only by the spherical wave effect, i.e., $K = \infty$. The emulation error due to a limited number of probes is not present. The error produced by the spherical wave effect decreases as R increases, as expected. The error for $R = 0.5$ m is below 0.1 for both frequencies. Fig. 5 demonstrates the impact of using a small anechoic chamber and limited number of probes on channel emulation accuracy. The curve labeled as $K = \infty$, $R = 0.5$ m represents the error due to the spherical wave effect. On the other hand, the curves labeled with $R = \infty$ show the emulation error due to the limited number of probes in an ideal setup. As we can see, the improvement of using a larger anechoic chamber generally diminishes as frequency increases for $K = 8$ and $K = 16$. This is because the test area increases with respect to the wavelength, causing the emulation accuracy to deteriorate regardless of the chamber size [2]. With $K = 8$, the emulation accuracy in terms of RMS error in an ideal setup ($R = \infty$) improves around 0.064 at 751 MHz and 0.01 at 2655 MHz, compared to results in a setup with $R = 0.5$ m. With $K = 16$, the improvement is 0.064 at 751 MHz and 0.08 at 2655 MHz.

C. Validation of the Chamber Compensation Technique

We will use the example shown in Fig. 3, where an undesired reflection exists when probe 1 is active. Fig. 6 shows the amplitude of the target field \mathbf{T} , distorted field \mathbf{S} , and compensated field for only probe 1 active. The target field has spherical wave front due to the small size of the chamber. Due to the reflection, the field within the test area is distorted,

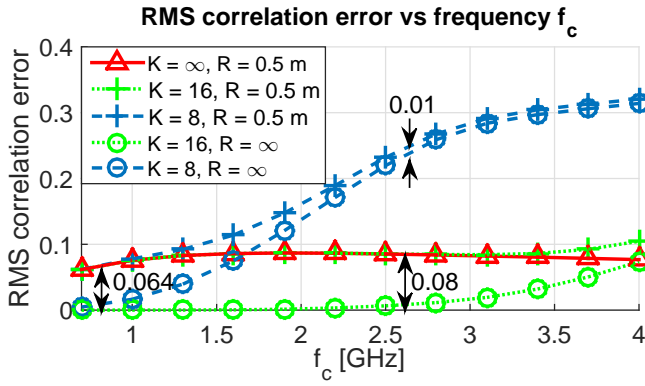


Fig. 5. RMS error for the SCME Urban micro channel model as a function of carrier frequency. Deviation between ideal and small setups are marked at 751 MHz and 2655 MHz.

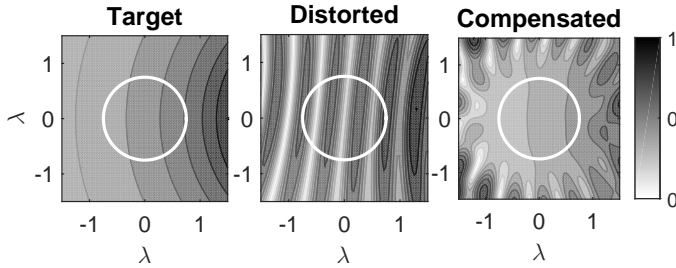


Fig. 6. Compensation of a static wave. White circle represents the test area. $R = 0.5$ m, $r = 0.1$ m, $K = 16$, $f = 2$ GHz.

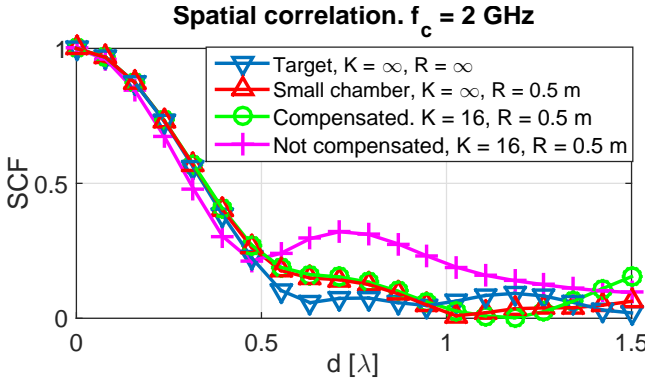


Fig. 7. Spatial Correlation Function (SCF) for the SCME Urban micro model, DUT placed along the y axis.

i.e., there is a fading pattern over space caused by the coherent summation of the target field and the reflection. The distortion caused by the reflection is compensated inside the test area using the proposed technique as shown in Fig. 6.

Once proven that the field within the test area can be compensated for a simple case, we calculate the channel coefficients for the SCME urban micro model. The spatial correlation emulated using the original channel coefficients and the compensated ones are calculated, and shown in Fig. 7. The target spatial correlation is calculated as in (1) using planar wave assumption. If the compensation technique is not applied, the reflection distorts the field in the test area and deteriorates the emulated spatial correlation. On the other hand, applying the compensation technique minimizes these effects and reduces the deviation considerably.

V. CONCLUSION AND FUTURE WORK

In this paper, we have investigated the feasibility of channel emulation in a small MPAC setup with the purpose of decreasing the cost of such setups and saving space. A OTA ring with radius $R = 0.5$ m has been considered in the simulations, which is less than half the size of other reported setups in the literature. Simulation results demonstrated that the error caused by the spherical wave effect is slightly worse for a chamber with $R = 0.5$ m compared to that with $R = 2.5$ m. Moreover, the emulation error caused by the use of a limited number of probes becomes dominant as the frequency increases, regardless of the ring size. Finally, we demonstrated that the proposed compensation technique can effectively minimize undesired effects such as reflections or coupling that might exist in small anechoic chambers. A spatial correlation error values below 0.1 is achieved using $K = 16$ probes when a strong reflection exists.

Some logic extensions could follow the work presented in this paper. The compensation technique was proposed for a 2D setup, yet in principle it would be applicable to a 3D setup as well. Throughout this paper, we have considered a RMS deviation up to 0.1 in the spatial correlation as a measure. However, it would be of interest to see the effect of the chamber size on other parameters, e.g., channel capacity. Furthermore, many practical aspects have been left for further study, e.g., design of the probe antennas, chamber design, measurement uncertainty levels in small MPAC setups, etc.

ACKNOWLEDGMENT

This work has been supported by the Danish High Technology Foundation via the VIRTUOSO project.

REFERENCES

- [1] P. Kyösti, T. Jämsä, and J.-P. Nuutinen, "Channel modelling for multi-probe over-the-air MIMO testing," *International Journal of Antennas and Propagation*, vol. 2012, 2012.
- [2] A. Khatun, T. Laitinen, V.-M. Kolmonen, and P. Vainikainen, "Dependence of error level on the number of probes in over-the-air multiprobe test systems," *International Journal of Antennas and Propagation*.
- [3] W. Fan, I. J. Szini, M. D. Foegelle, J. Ø. Nielsen, and G. F. Pedersen, "Measurement uncertainty investigation in the multi-probe OTA setups," in *Antennas and Propagation (EuCAP), 2014 8th European Conference on*, April 2014, pp. 1068–1072.
- [4] SATIMO, "StarMIMO." [Online]. Available: <http://www.satimo.com/content/products/starmimo-hu>
- [5] A. Alayon Glazunov, S. Prasad, P. Handel, T. Bolin, and K. Prytz, "Impact of scattering within a multipath simulator antenna array on the Ricean fading distribution parameters in OTA testing," *IEEE Transactions on Antennas and Propagation*, vol. 62, no. 6, pp. 3257–3269, March 2014.
- [6] T. Hansen, "Plane wave generation within a small volume of space for evaluation of wireless devices," U.S. Patent 2013/0052962, Aug. 8, 2012.
- [7] P. Kyösti and L. Hentilä, "Criteria for physical dimensions of MIMO OTA multi-probe test setup," in *6th European Conference on Antennas and Propagation (EuCAP)*, March 2012, pp. 2055–2059.
- [8] W. Fan, X. Carreño, F. Sun, J. Ø. Nielsen, M. B. Knudsen, and G. F. Pedersen, "Emulating spatial characteristics of MIMO channel for OTA testing," *IEEE Transactions on Antennas and Propagation*, vol. 61, no. 8, pp. 4306–4314, May 2013.
- [9] D. Parvegi, T. Laitinen, A. Khatun, V.-M. Kolmonen, and P. Vainikainen, "Calibration procedure for 2-D MIMO over-the-air multi-probe test system," in *6th European Conference on Antennas and Propagation (EuCAP)*, March 2012, pp. 1594–1598.